



Performance and longevity of CO₂ based mixtures in CMS improved Resistive Plate Chambers in the HL-LHC environment



J.P. Pinheiro ⁴*, M. Tytgat ¹, a, K. Mota Amarilo ², b, A. Samalan ², c, K. Skovpen ², G.A. Alves ³, E. Alves Coelho ³, F. Marujo da Silva ³, M. Barroso Ferreira Filho ⁴, E.M. Da Costa ⁴, D. De Jesus Damiao ⁴, B.C. Ferreira ⁴, S. Fonseca De Souza ⁴, L. Mundim ⁴, H. Nogima ⁴, A. Santoro ⁴, M. Thiel ⁴, R. Gomes De Souza ⁴, T. De Andrade rangel Monteiro ⁴, A. Aleksandrov ⁵, R. Hadjiiska ⁵, P. Iaydjiev ⁵, M. Shopova ⁵, G. Sultanov ⁵, A. Dimitrov ⁶, L. Litov ⁶, B. Pavlov ⁶, P. Petkov ⁶, A. Petrov ⁶, E. Shumka ⁶, P. Cao ⁷, W. Diao ⁷, W. Gong ⁷, Q. Hou ⁷, H. Kou ⁷, Z.-A. Liu ⁷, J. Song ⁷, N. Wang ⁷, J. Zhao ⁷, S.J. Qian ⁸, C. Avila ⁹, D.A. Barbosa Trujillo ⁹, A. Cabrera ⁹, C.A. Florez ⁹, J.A. Reyes Vega ⁹, R. Aly ^{10,12}, d, A. Radi ¹¹, e, Y. Assran ¹², f, I. Crotty ¹³, M.A. Mahmoud ¹³, L. Balleyguier ¹⁴, X. Chen ¹⁴, C. Combaret ¹⁴, G. Galbit ¹⁴, M. Gouzevitch ¹⁴, G. Grenier ¹⁴, I.B. Laktineh ¹⁴, A. Luciol ¹⁴, L. Mirabito ¹⁴, W. Tromeur ¹⁴, I. Bagaturia ¹⁵, O. Kemularia ¹⁵, I. Lomidze ¹⁵, Z. Tsamalaidze ¹⁵, g, V. Amoozegar ¹⁶, B. Boghrati ¹⁶, M. Ebrahimi ¹⁶, F. Esfandi ¹⁶, Y. Hosseini ¹⁶, M. Mohammadi Najafabadi ¹⁶, E. Zareian ¹⁶, M. Abbrescia ^{17,18}, N. De Filippis ^{17,19}, G. Iaselli ^{17,19}, F. Loddo ¹⁷, G. Pugliese ^{17,19}, D. Ramos ¹⁷, L. Benussi ²⁰, S. Bianco ²⁰, S. Meola ²⁰, h, D. Piccolo ²⁰, S. Buontempo ²¹, F. Carnevali ^{21,22}, L. Lista ^{21,22}, i, P. Paolucci ²¹, j, F. Fienga ²³, A. Braghieri ²⁴, P. Montagna ^{24,25}, C. Riccardi ^{24,25}, P. Salvini ²⁴, P. Vitulò ^{24,25}, T.J. Kim ²⁶, E. Asilar ²⁶, Y. Ryou ²⁶, S. Choi ²⁷, B. Hong ²⁷, K.S. Lee ²⁷, J. Goh ²⁸, J. Shin ²⁸, Y. Lee ²⁹, I. Pedraza ³⁰, C. Uribe Estrada ³⁰, H. Castilla-Valdez ³¹, R. Lopez-Fernandez ³¹, A. Sánchez Hernández ³¹, M. Ramírez García ³², D.L. Ramirez Guadarrama ³², M.A. Shah ³², E. Vazquez ³², N. Zaganidis ³², A. Ahmad ³³, M.I. Asghar ³³, H.R. Hoorani ³³, S. Muhammad ³³, L.E. Sánchez ³⁴, J. Eysermans ³⁵, on behalf of the CMS Collaboration

¹ Vrije Universiteit Brussel, Brussel, Belgium² Universiteit Gent, Gent, Belgium³ Centro Brasileiro de Pesquisas Fisicas, Rio de Janeiro, Brazil⁴ Universidade do Estado do Rio de Janeiro, Rio de Janeiro, Brazil^{*} Corresponding author.E-mail address: joao.pedro.gomes.pinheiro@cern.ch (J.P. Pinheiro).^a Also at Ghent University, Ghent, Belgium.^b Now at UERJ, Rio de Janeiro, Brazil.^c Now at PSI, Villigen, Switzerland.^d Also at Academy of Scientific Research and Technology of the Arab Republic of Egypt, Egyptian Network of High Energy Physics, Cairo, Egypt.^e Also at Sultan Qaboos University, Muscat, Oman.^f Also at Suez University, Suez, Egypt.^g Also at an institute or an international laboratory covered by a cooperation agreement with CERN.^h Also at Università degli Studi Guglielmo Marconi, Roma, Italy.ⁱ Also at Scuola Superiore Meridionale, Università di Napoli 'Federico II', Napoli, Italy.^j Also at CERN, European Organization for Nuclear Research, Geneva, Switzerland.

⁵ Institute for Nuclear Research and Nuclear Energy, Bulgarian Academy of Sciences, Sofia, Bulgaria
⁶ Faculty of Physics, University of Sofia, Sofia, Bulgaria
⁷ Institute of High Energy Physics and University of the Chinese Academy of Sciences, Beijing, China
⁸ School of Physics, Peking University, Beijing, China
⁹ Universidad de Los Andes, Bogota, Colombia
¹⁰ Physics Department, Faculty of science, Helwan University, Cairo, Egypt
¹¹ Department of Physics, Faculty of Science, Ain Shams University, Cairo, Egypt
¹² The British University in Egypt, Cairo, Egypt
¹³ Center for High Energy Physics (CHEP-FU), Fayoum University, El-Fayoum, Egypt
¹⁴ Institut de Physique des 2 Infinis de Lyon, Villeurbanne, France
¹⁵ Georgian Technical University, Tbilisi, Georgia
¹⁶ Institute for Research in Fundamental Sciences, Tehran, Iran
¹⁷ INFN Sezione di Bari, Bari, Italy
¹⁸ Università di Bari, Bari, Italy
¹⁹ Politecnico di Bari, Bari, Italy
²⁰ INFN Laboratori Nazionali di Frascati, Frascati, Italy
²¹ INFN Sezione di Napoli, Napoli, Italy
²² Università di Napoli 'Federico II', Napoli, Italy
²³ Dipartimento di Ingegneria Elettrica e delle Tecnologie dell'Informazione - Università Degli Studi di Napoli Federico II, Napoli, Italy
²⁴ INFN Sezione di Pavia, Pavia, Italy
²⁵ Università di Pavia, Pavia, Italy
²⁶ Hanyang University, Seoul, Republic of Korea
²⁷ Korea University, Seoul, Republic of Korea
²⁸ Kyung Hee University, Department of Physics, Seoul, Republic of Korea
²⁹ Sungkyunkwan University, Suwon, Republic of Korea
³⁰ Benemerita Universidad Autónoma de Puebla, Puebla, Mexico
³¹ Centro de Investigacion y de Estudios Avanzados del IPN, Mexico City, Mexico
³² Universidad Iberoamericana, Mexico City, Mexico
³³ National Centre for Physics, Quaid-I-Azam University, Islamabad, Pakistan
³⁴ University of Dundee, Dundee, Scotland, United Kingdom
³⁵ Massachusetts Institute of Technology, Cambridge, MA, USA

ARTICLE INFO

Keywords:

Gaseous detectors
 Resistive Plate Chambers
 Eco-friendly gas mixtures

ABSTRACT

Resistive Plate Chamber (RPC) detectors are widely used in high-energy physics experiments. In the Compact Muon Solenoid (CMS), the RPC gas mixture is composed of 95.2% $\text{C}_2\text{H}_2\text{F}_4$, which generates a large number of ion-electron pairs, 4.5% iC_4H_{10} to suppress photon feedback effects, and 0.3% SF_6 as an electron quencher to ensure operation in streamer-free mode. Given the high global warming potential (GWP) of $\text{C}_2\text{H}_2\text{F}_4$ at 1430 and the recent reduction in the emission of F gases imposed by the European Union, efforts have intensified in recent years to explore environmentally friendly gas alternatives. A promising short- to mid-term solution for the upcoming years of Large Hadron Collider (LHC) operations is to lower the GWP of the RPC gas mixture by partially substituting $\text{C}_2\text{H}_2\text{F}_4$ with CO_2 . The performance tests of the alternative gas mixtures are conducted at the CERN Gamma Irradiation Facility (GIF++) in the North Area of the Super Proton Synchrotron (SPS), where a 13.6 TBq radiation source and an SPS muon beam simulate the High-Luminosity (HL) Phase II conditions of the LHC. This paper reports on the performance of a 1.4 mm gap RPC using three different CO_2 -based mixtures under intense gamma radiation, with the first results on the longevity campaign.

1. Introduction

The CMS Muon System comprises four types of gaseous detectors: Drift Tubes (DT) in the barrel region, Cathode Strip Chambers (CSC) and Gas Electron Multipliers (GEM) in the endcaps, and Resistive Plate Chambers (RPC) in both the barrel and endcap areas, providing coverage up to a pseudorapidity of $|\eta| = 2.4$ [1]. The current RPC system includes 1056 chambers, each with a double 2 mm gas gap, and has consistently operated with high efficiency since CMS began collecting data [2]. In preparation for the Phase-II upgrade of the LHC [3], new improved RPCs (iRPCs) will be installed in the forward region of CMS, as depicted in Fig. 1. These iRPCs also employ double-gap configurations but feature narrower 1.4 mm gas gaps and 1.4 mm thick High Pressure Laminate (HPL) electrodes. Additionally, they are equipped with new Front-End Boards (FEB) capable of setting a charge threshold as low as 30 fC, a significant improvement over the 150 fC threshold of the existing RPC detectors [4].

The standard CMS-RPC gas mixture consists of 95.2% $\text{C}_2\text{H}_2\text{F}_4$, which generates a high number of ion-electron pairs, 4.5% iC_4H_{10} to suppress photon-feedback effects, and 0.3% SF_6 as an electron quencher to ensure operation in streamer-free mode [2]. The European Union has set ambitious targets to reduce greenhouse gas (GHG) emissions,

such as those from $\text{C}_2\text{H}_2\text{F}_4$, by 55% by 2030 and to achieve net-zero emissions by 2050 [5]. CERN is addressing these regulations, noting that 90% of its direct emissions are from experiments, and approximately 78% of its GHG emissions result from using F-gases [6]. It is essential for the future of RPC detectors to find a permanent replacement for $\text{C}_2\text{H}_2\text{F}_4$, while also exploring the feasibility of mid-term solutions to reduce fluorinate gases (F-gases) emissions maintaining the performance of the detectors and ensuring long term operation.

Several strategies have been explored to reduce the emission of GHG in CMS-RPC, such as the implementation of a gas recirculation system [7], the repair of leaky chambers, and the development of a gas recuperation system [8]. In parallel, many R&D studies have also been undertaken to find a replacement for $\text{C}_2\text{H}_2\text{F}_4$. This paper is a follow-up of [9], aiming to find a short-to-mid-term solution for reducing $\text{C}_2\text{H}_2\text{F}_4$ emissions by replacing it with CO_2 . The studies are carried out at the GIF++ Facility at CERN with an iRPC prototype.

2. Gamma irradiation facility and the experimental setup

The GIF++ Facility in the North Area of the SPS features a ^{137}Cs source with adjustable filters to vary gamma intensity and a high energy muon beam (100 GeV/c) from the SPS H4 beamline [10]. The ^{137}Cs source, emitting 662 keV photons, closely matches the neutron-induced background energy spectrum expected at CMS during Phase II of the LHC.

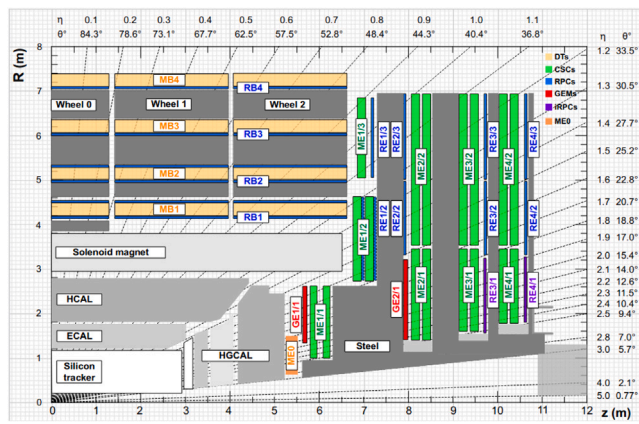


Fig. 1. Muon System of the Compact Muon Solenoid for the Phase-II upgrade of LHC. Existing RPCs are represented in blue. The new iRPC to be installed in the stations RE3/1 and RE4/1 are represented in purple [1].

In early 2023, an iRPC prototype was installed in Gif++ to test various CO_2 -based gas mixtures. The chamber, with two $50 \times 50 \text{ cm}^2$ gaps of 1.4 mm width and 1.4 mm thick electrodes, uses 16 signal readout strips. A custom FEB with a 20Ω input impedance, 200 gain, 60 ns signal width, and a 500 μV threshold (around 60 fC charge equivalent) was used. Signal processing is handled by a CAEN TDC V1190 A, with a triggering system using four scintillators. The trigger setup is composed of two scintillators outside the Gif++ bunker and two scintillators inside the bunker, resulting in an effective area of approximately $10 \times 10 \text{ cm}^2$.

The muon window, determined from a Gaussian fit of the muon signal ($2 \times 3 \times \sigma$), is expected to be from 50 to 75 ns. This value is mainly driven by: TDC trigger gate frequency, strip (FEB channel) offsets, TDC channel offsets, etc. In background-free conditions, efficiency is defined as the ratio of detected events within the muon window to the total number of muon triggers. Under gamma radiation background, we estimate a window outside the muon window (blue dashed area in Fig. 2) as the background/noise window. Bayesian correction is applied in order to subtract the gamma contribution inside the muon window:

$$\epsilon_{\text{muon}} = \frac{\epsilon_{\text{total}} - \epsilon_{\gamma}}{1 - \epsilon_{\gamma}} \quad (1)$$

where ϵ_{muon} is the corrected efficiency, ϵ_{total} the total hit efficiency (all hits inside muon window), and ϵ_{γ} the gamma efficiency in the area outside the muon window. A dedicated clustering algorithm groups hits on adjacent strips within a 30 ns time window to construct the muon/gamma cluster.

The Gif++ gamma source uses an advanced filter system for independent gamma rate control in upstream and downstream areas. To simulate HL-LHC conditions, where the background rate is expected to be around 600 Hz/cm^2 , the iRPC chambers are placed in the upstream area and data is collected at rates from a few Hz/cm^2 to 2 kHz/cm^2 , incorporating a safety factor of 3 [12].

Efficiency (ϵ) is measured at various high voltages (HV_{eff}) to generate the S-curve, modeled using the equation:

$$\epsilon = \frac{\epsilon_{\text{max}}}{1 + e^{-\lambda(HV_{\text{eff}} - HV_{50\%})}} \quad (2)$$

where ϵ_{max} is the plateau efficiency, λ is a scaling factor related to the slope, and $HV_{50\%}$ is the voltage at 50% efficiency. The chamber's working point (WP) is set where efficiency reaches 95%, with an extra 150 V margin to achieve the plateau.

The effective HV is corrected by environmental parameters, as pressure (P) and temperature (T), giving the applied HV:

$$HV_{\text{app}} = HV_{\text{eff}} \left[(1 - \alpha) + \alpha \frac{P}{P_0} \frac{T_0}{T} \right] \quad (3)$$

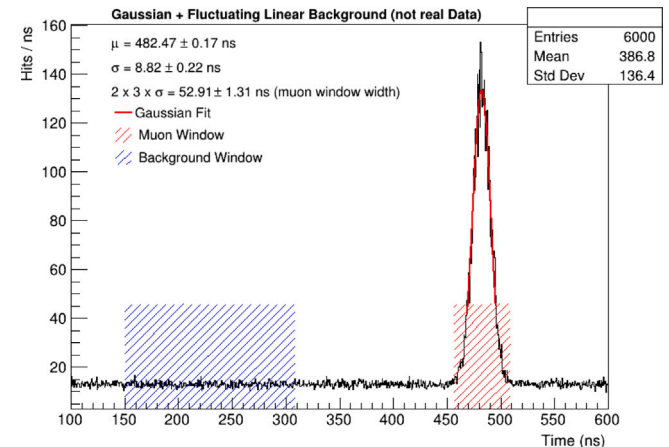


Fig. 2. Definition of muon window and gamma window for efficiency calculation. This plot represents random data for didactic purposes [11].

Table 1

Table displaying the composition of the gas mixtures utilized, alongside the standard RPC gas mixture in CMS. The final column shows the equivalent emissions in tons of CO_2 , which are around 15%–26% lower for the alternative CO_2 -based mixtures examined in this study.

Mixtures	$\text{C}_2\text{H}_2\text{F}_4$	CO_2	$\text{i-C}_4\text{H}_{10}$	SF_6	$\text{CO}_2^{\text{equiv}}$ (t)
STD	95.2%	0	4.5	0.3	664
MIX1	64%	30%	5%	1%	565
MIX2	54%	40%	5%	1%	500
MIX3	64.5%	30%	5%	0.5%	494

where $P_0 = 990 \text{ mbar}$, $T_0 = 293.15 \text{ K}$ and $\alpha = 0.8$ are the reference values, following [13].

3. Alternative CO_2 -based mixtures

Various alternatives to $\text{C}_2\text{H}_2\text{F}_4$ are still being investigated, with tetrafluoropropene HFO-1234ze ($\text{C}_3\text{H}_2\text{F}_4$) emerging as one of the most promising candidates [14]. This low-global-warming-potential refrigerant has already been adopted by the industry as a replacement for $\text{C}_2\text{H}_2\text{F}_4$. However, when used in RPCs, HFO-1234ze alone does not provide optimal performance, as it tends to increase the operating voltage. To reduce the working point, CO_2 is introduced in varying percentages for testing [15]. To mitigate the increase in streamer probability led by the addition of CO_2 , the concentration of SF_6 is increased up to 1% SF_6 [16]. These adjustments help maintain the desired detector efficiency and stability under high-background conditions.

Meanwhile, the RPC community has adopted additional strategies. Since 2023, the ATLAS-RPC system has started replacing 30% of $\text{C}_2\text{H}_2\text{F}_4$ with CO_2 , however increasing SF_6 up to 1%. The trigger efficiency and cluster size remain comparable to those of the standard gas mixture, though the currents have been observed to increase, prompting ongoing longevity studies [17]. In the present paper, three CO_2 -based mixtures are tested, as presented in Table 1. The equivalent emissions in tons of CO_2 are around 15%–26% lower with respect to the standard gas mixture. The performance of the different gas mixtures tested is presented in Section 4 and the first longevity results are presented in Section 5 after irradiation campaign with MIX1.

4. Performance results

In the view of performance assurance of the iRPC prototype, scans with the standard gas mixture were taken with different background gamma rates, as shown in Fig. 3. The working point is around 7.2 kV and efficiency of 98% in the absence of gamma background, as expected for a double gap 1.4 mm iRPC [4], while the efficiency drop

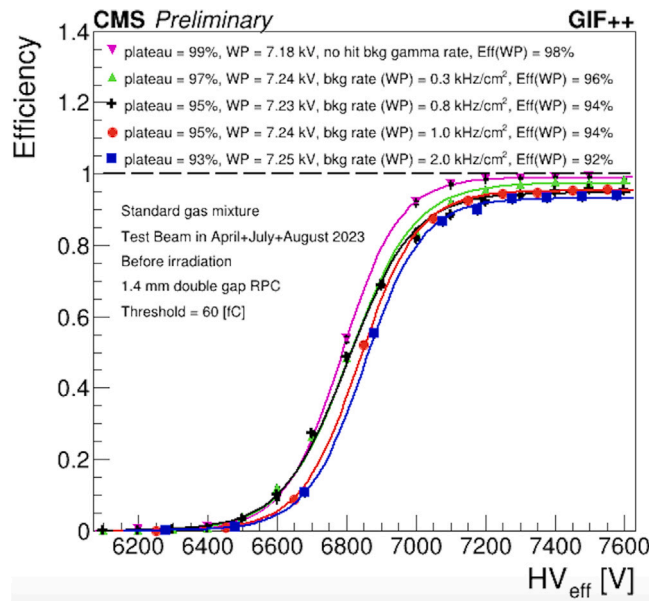


Fig. 3. Efficiency scans with standard gas mixture with the iRPC prototype before the irradiation campaign [11].

of 6% with the background rate up to 2 kHz/cm^2 is expected mainly due to the electronics prototype dead time of around 80 ns.

Efficiency scans were conducted without background rate for the various gas mixtures listed in Table 1. As illustrated in Fig. 4, the efficiency remains consistent across all tested mixtures, while the working point varies depending on the concentrations of CO_2 and SF_6 . CO_2 , being a low-density inert gas, shifts the working point to lower values, whereas SF_6 , a gas with high electronegativity, raises the working point. The two mixtures containing 30% CO_2 and 0.5% SF_6 exhibit a similar working point compared to the mixture with 40% CO_2 and 1.0% SF_6 . Nevertheless, all tested gas mixtures have a lower working point relative to the standard mixture.

The efficiency of different gas mixtures, measured under a background gamma rate of 800 Hz/cm^2 —similar to the expected conditions for iRPC chambers at the HL-LHC—is presented in Fig. 5. The slight drop in efficiency observed in CO_2 -based mixtures can be attributed to the lower density of these mixtures compared to the standard one. This reduced density decreases the probability of ionizing interactions between the incoming muon and the gas molecules, affecting the efficiency particularly at higher rates. However, this effect is not pronounced for MIX1 and MIX3, which contain 30% CO_2 , indicating that moderate increases in CO_2 content do not significantly compromise the detector's performance.

Fig. 6 presents the muon cluster size as a function of the effective high voltage relative to the working point ($\text{HV}_{\text{eff}} - \text{HV}_{\text{WP}}$) for different gas mixtures tested. The variations in cluster size across these mixtures are minimal, demonstrating that the iRPC chambers maintain comparable performance to the standard mixture even with increased CO_2 gas component. This stability in cluster size may be attributed to the presence of SF_6 , which compensates for the effects of reduced density from CO_2 . Notably, even with only 0.5% SF_6 , the cluster size remains consistent with that of the standard gas mixture, highlighting the effectiveness of SF_6 in preserving detector performance.

5. Longevity results

Following the performance verification, a dedicated longevity campaign was conducted using MIX1, the gas mixture containing 30% CO_2 and 1.0% SF_6 . The detector was maintained at its working point in the bunker and continuously flushed with the CO_2 -based mixture while

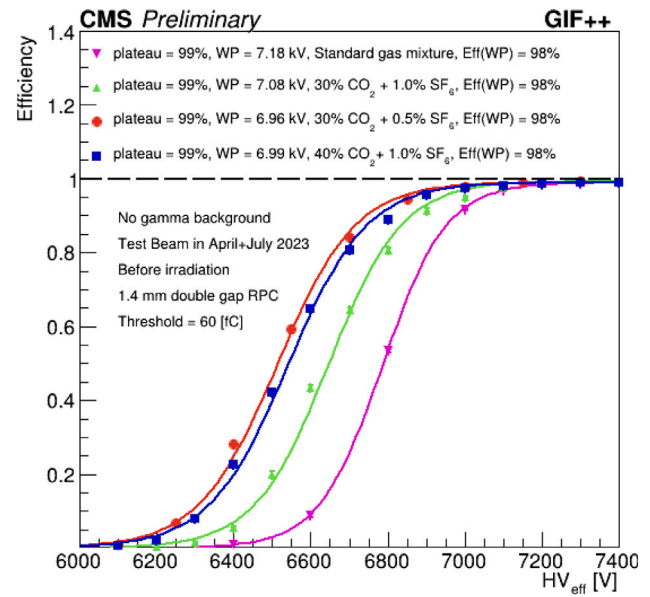


Fig. 4. Efficiency scans with different gas mixtures without gamma background with the iRPC prototype before the irradiation campaign [11].

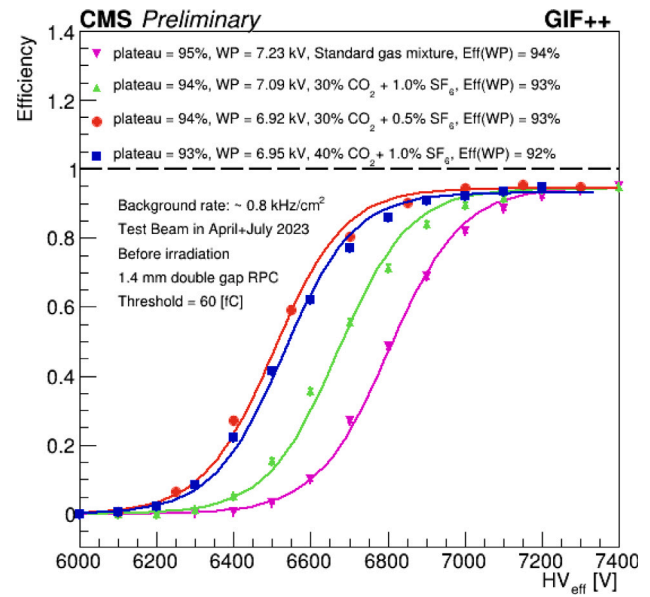


Fig. 5. Efficiency scans with different gas mixtures with a gamma background of 800 Hz/cm^2 with the iRPC prototype before the irradiation campaign [11].

accumulating charge. The total charge accumulated was measured based on the current over time of the chamber. Between 2023 and 2024, the detector successfully accumulated 40 mC/cm^2 , representing 5% of the total charge expected by the end of CMS operation, which is 1 C/cm^2 , including a safety factor of 3 [12].

The working points exhibit minimal variation with increasing background gamma rates, as shown in Fig. 7. The limited impact of the ohmic contribution can be attributed to the relatively small size of the detector and the resistivity of the HPL plates on the order of $1.2 \times 10^{10} \Omega \text{ cm}$. The average working point when we compare the results before and after the radiation campaign shows a small increase of 30 V, with no impact on the chamber performance. The difference in the working point due to the balance of CO_2 and SF_6 remains the same. The resistivity of the electrodes was monitored throughout the aging test, and no significant variations were observed.

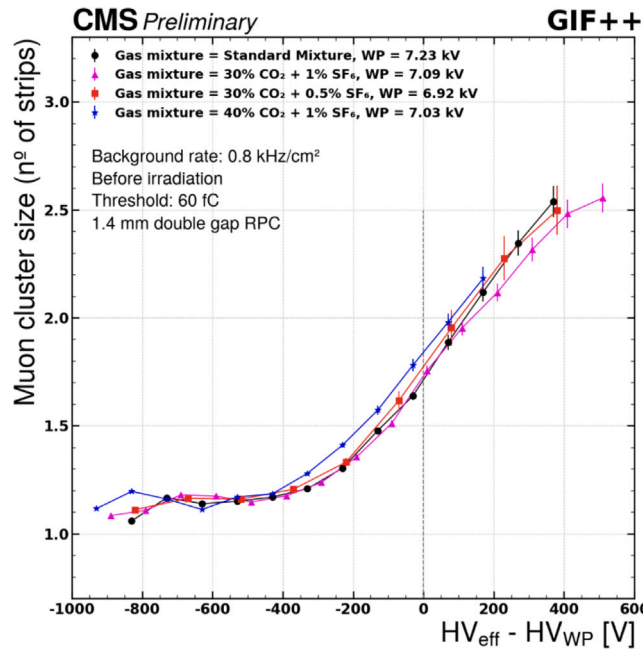


Fig. 6. Muon cluster size for different gas mixtures at 800 Hz/cm² of background gamma rate before the irradiation campaign [11].

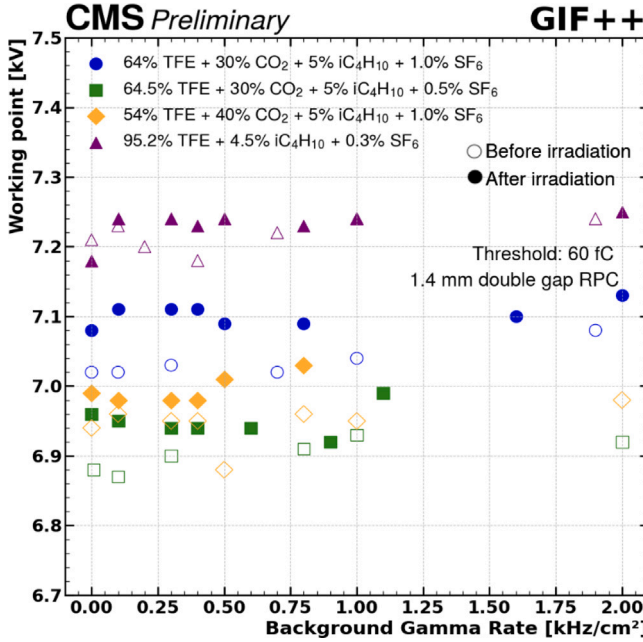


Fig. 7. Working point as a function of background gamma rates of different gas mixtures before and after the irradiation campaign. A small change in working point is observed [11].

Fig. 8 shows the efficiency at the working point as a function of the background gamma rate for the gas mixtures tested. The performance remains comparable across all gas mixtures under moderate radiation conditions. However, under extreme radiation rates, a decline in efficiency to values below 90% was observed after irradiation. Since this drop occurred across all tested gas mixtures, further studies are ongoing to understand whether this drop is linked to the limitations of the electronics prototype, which was not designed to operate under such high radiation levels.

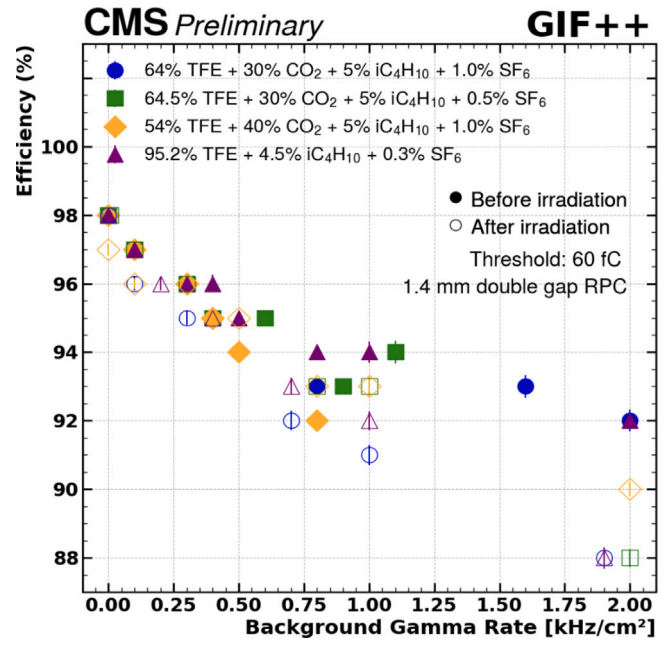


Fig. 8. Efficiency at WP as a function of background gamma rates of different gas mixtures before and after the irradiation campaign. The drop in efficiency observed in extreme background gamma rates may be explained by electronics limitation [11].

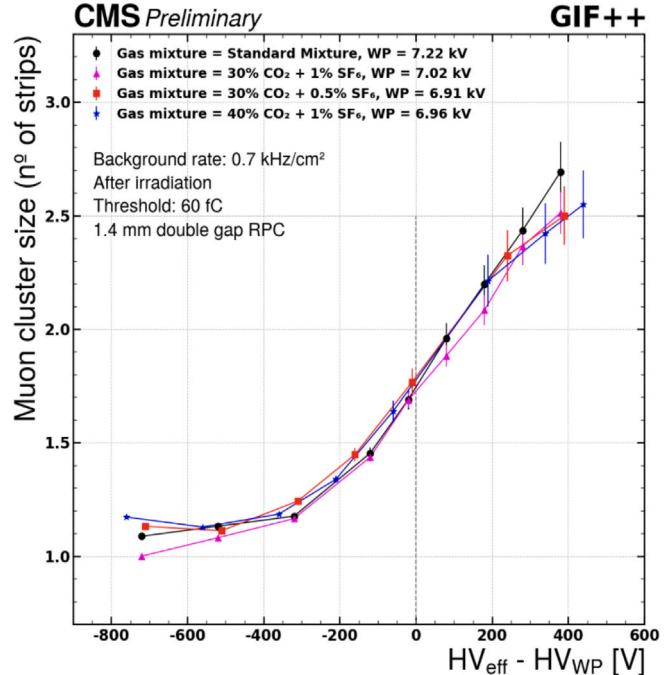


Fig. 9. Muon cluster size for different gas mixtures at 700 Hz/cm² of background gamma rate after the irradiation campaign [11].

As shown in Fig. 9, the muon cluster size at 700 Hz/cm² remains consistent for all tested gas mixtures, even after the radiation campaign. This is in agreement with the pre-irradiation average of 1.7 strips, as shown in Fig. 6.

As reported in previous studies [9], the current in the gas gaps is expected to be around 20% higher for CO_2 -based mixtures, in comparison with the standard one. However, as shown in Fig. 10, negligible changes were observed after the irradiation campaign.

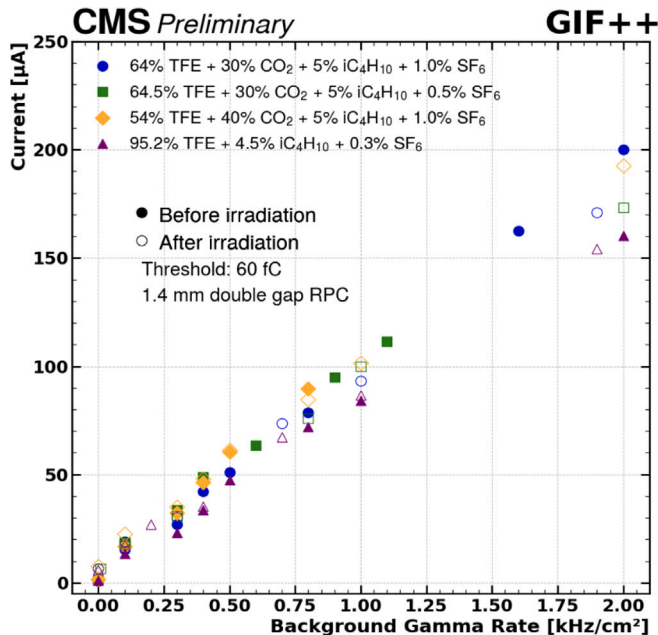


Fig. 10. Currents at the working point as a function of the background gamma rate of different gas mixtures before and after the irradiation campaign. For all CO_2 -based mixtures, the current at the working point is around 20% higher than the standard gas mixture, but negligible changes after irradiation have been observed [11].

6. Conclusion

The results presented in this paper demonstrate that CO_2 -based gas mixtures are a promising alternative to the standard RPC gas mixture for use in the CMS detector at the HL-LHC. The iRPC prototype exhibited robust performance across various background gamma rates, with minimal efficiency loss and stable cluster size. Nevertheless, the observed efficiency drop under extreme radiation conditions highlights the need for further investigation into the limitations of the current electronics prototype. The irradiation campaign will continue, and future studies will prioritize optimizing the electronics and exploring MIX3, which offers lower CO_2 equivalent emissions. Additionally, upcoming tests will include 2 mm double-gap RPCs, representative of the 1056 chambers present in CMS, to ensure that performance is met for large-scale implementation.

Declaration of competing interest

The authors declare the following financial interests/personal relationships which may be considered as potential competing interests: Joao Pedro Gomes Pinheiro reports financial support was provided by

National Council for Scientific and Technological Development. Joao Pedro Gomes Pinheiro reports financial support was provided by Carlos Chagas Filho Foundation for Research Support of Rio de Janeiro State. Joao Pedro Gomes Pinheiro reports financial support was provided by Coordination of Higher Education Personnel Improvement. If there are other authors, they declare that they have no known competing financial interests or personal relationships that could have influenced the work reported in this paper.

Acknowledgments

We acknowledge the support for the CMS detector from the funding agencies: FWO (Belgium); CNPq, Brazil, CAPES, FAPERJ (Brazil); MES, BNSF (Bulgaria); CERN; CAS, MoST, NSFC (China); MINCIENCIAS (Colombia); CEA, CNRS/IN2P3 (France); SRNSFG (Georgia); IPM (Iran); INFN (Italy); MSIP, NRF (Korea); BUAP, CINVESTAV, CONACYT, LNS, SEP, UASLP-FAI (Mexico); PAEC (Pakistan); DOE, NSF (USA).

References

- [1] C.M.S. Collaboration, JINST 3 (2008) S08004, <http://dx.doi.org/10.1088/1748-0221/3/08/S08004>.
- [2] M.A. Shah, et al., JINST 14 (2019) C11012, <http://dx.doi.org/10.1088/1748-0221/14/11/C11012>.
- [3] A. Hayrapetyan, et al., CMS Collaboration, Development of the CMS detector for the CERN LHC Run 3, JINST 19 (05) (2024) P05064, <http://dx.doi.org/10.1088/1748-0221/19/05/P05064>, arXiv:2309.05466.
- [4] J.P.G. Pinheiro, et al., CMS Muon Collaboration, Nucl. Instrum. Meth. A 1069 (2024) 169923, <http://dx.doi.org/10.1016/j.nima.2024.169923>.
- [5] European Commission, The European Green Deal, 2024, . (Accessed 12 November 2024).
- [6] CERN, CERN Environment Report 2021–2022: Emissions, 2024, . (Accessed 12 November 2024).
- [7] A. Gelmi, R. Guida, B. Mandelli, J. Instrum. 16 (04) (2021) C04004, <http://dx.doi.org/10.1088/1748-0221/16/04/C04004>.
- [8] M. Arena, et al., Nucl. Instrum. Meth. A 1068 (2024) 169789, <http://dx.doi.org/10.1016/j.nima.2024.169789>.
- [9] J.P.G. Pinheiro, et al., CMS Muon Group Collaboration, Nucl. Instrum. Meth. A 1065 (2024) 169474, <http://dx.doi.org/10.1016/j.nima.2024.169474>.
- [10] D. Pfeiffer, et al., Nucl. Instrum. Meth. A 866 (2017) 91.
- [11] CMS Collaboration, CO_2 -based mixture for iRPC detector studies, 2024, URL <https://cds.cern.ch/record/2916753>.
- [12] T. Hebbeker, A. Korytov, CMS Collaboration, The Phase-2 Upgrade of the CMS Muon Detectors, 2017.
- [13] T. Abdelhameid, et al., Nucl. Instrum. Meth. A 1059 (2024) 168957, <http://dx.doi.org/10.1016/j.nima.2023.168957>.
- [14] G. Rigoletti, et al., PoS (2020) 164, <http://dx.doi.org/10.22323/1.364.0164>.
- [15] G. Rigoletti, R. Guida, B. Mandelli, Eur. Phys. J. Plus 138 (2023) 841, <http://dx.doi.org/10.1140/epjp/s13360-023-04434-y>, URL <https://link.springer.com/article/10.1140/epjp/s13360-023-04434-y>.
- [16] D.R. López, et al., Nucl. Instrum. Meth. A 1069 (2024) 169950, <http://dx.doi.org/10.1016/j.nima.2024.169950>.
- [17] E. Ballabene, ATLAS Collaboration, Performance of ATLAS RPC detectors and L1 Muon Barrel Trigger with a new CO_2 -based gas mixture, 2024, URL